The International Supercritical CO_2 Energy Technologies Symposium
March 2 - 5, 2026, Pittsburgh, PA
Paper #054

Aeromechanics Considerations for a Centrifugal Compressor Impeller operation in High Density Fluids

Authors: Manish Thorat, Hanxiang Jin, Brian Pettinato, Rob Pelton, Karl Wygant

Manish Thorat is a Senior Engineer and Machinery Dynamics & Acoustics Group Lead, R&D at Ebara Elliott Energy. He has been with Elliott since 2010. His areas of expertise include rotordynamics, vibration analysis, testing and evaluation of seal designs, squeeze film dampers and fluid film journal bearing design. Mr. Thorat holds three U.S. patents and has co-authored five publications in ASME journals. Mr. Thorat is a member of ASME and STLE. Mr. Thorat earned his MS degree in Mechanical Engineering from Texas A&M University (2010) and BE in Mechanical Engineering from Mumbai University (2007)

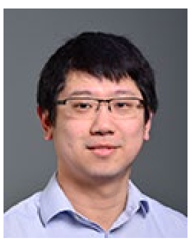

Hanxiang Jin joined Ebara Elliott Energy in February 2020 as a mechanical engineer in the Aero and Structural Dynamics Department, Solid Mechanics Group, in Jeannette, Pennsylvania. He received his Ph.D. from Virginia Tech in 2019. His research interests include solid mechanics, fluid mechanics, and rotordynamics.

Brian Pettinato is a Senior Manager of Aero and Structural Dynamics at Ebara Elliott Energy in Jeannette, Pennsylvania. He has been with Elliott since 1995. His primary area of expertise is machinery dynamics. Prior to joining Elliott, he worked as a project engineer for CentriMarc. Mr. Pettinato received his B.S. (1989) and M.S. (1992) Mechanical Engineering degrees from the University of Virginia. He has coauthored over thirty technical papers and holds four U.S. patents. Mr. Pettinato is a fellow member of ASME, a member of STLE, and a registered Professional Engineer in the State of Pennsylvania. He serves on the Turbomachinery Advisory Committee of Texas A&M and on the API 684 rotordynamics task force.

Robert Pelton is the manager of the compressor aerodynamic design team in the research and development group at Ebara Elliott Energy. He oversees the technical team responsible for aerodynamic development and performance of new products, focusing on centrifugal compressors. Prior to coming to Elliott Group, Mr. Pelton worked at Samsung/Hanwha Power Systems where he focused on the development of the core turbomachinery for integrally geared compressors. He started his career at ConceptsNREC and gained experience there in the design of a wide range of turbomachinery. He holds a B.S. and M.S. in Mechanical Engineering from Brigham Young University.

Dr. Wygant is Sr. Manager of Advanced Technology Programs at Elliott Group. Dr. Wygant holds an M.S. and Ph.D. in Mechanical Engineering from the University of Virginia and an M.B.A. from Norwich University. His engineering experience over the last 25 years is related to a development of new turbomachinery products, including: rocket turbopumps, automotive turbochargers, industrial compressors, steam turbines, gas turbines, and novel turbomachinery applications.His management background includes: project management, multi-group management, business management, and leading new product development from inception to market delivery.

Abstract

Structural integrity of a centrifugal compressor impeller from aeromechanical failure modes is an important design consideration especially for operations with high density fluids. This paper provides an overview of typical aeromechanic failure modes of a centrifugal compressor impeller and design considerations for avoiding these failures.

A representative centrifugal compressor impeller stage with working fluid as CO_2 close to critical point is modeled using CFD. Excitation forces due to Impeller-Diffuser interaction are estimated using Non-Linear Harmonic (NLH) Method. Aerodynamic damping is assumed in the analysis. The excitation and damping are further used to estimate impeller stresses using forced harmonic response analysis. The structural integrity of the impeller is assessed using Fatigue analysis based on the estimated steady and cyclic stresses on the impeller.

Introduction

Aeromechanic failure modes in bladed turbomachinery applications can be characterized by two major failure mechanisms - forced excitation and flutter. In centrifugal compressor applications, typical failure modes seen are due to forced excitation from interaction resonances such as due to interaction between inlet guide vanes, return channel or diffuser vanes with impeller blades. Interactions due to rotating stall and unsteady flow at off-design operating conditions are reported by Haupt et al. ([1],[2]) and Engeda [3]. Acoustic interactions (See [5, 6]) can also be of significance especially in the secondary flow passages such as shroud and back-wall cavities of impeller stages. Failures due to flutter (loss of aerodynamic damping) are rare in centrifugal compressor applications although suspected cases are reported in literature (See Curtin et al. [4]). Prediction of aerodynamic damping is an important consideration for forced response evaluation. Kushner et al. [7] provide an extensive review of turbomachinery aeromechanics with case studies especially with centrifugal compressor impeller applications .

In sCO_2 applications, an important consideration is the rapid variation in gas properties in the supercritical region which may influence the estimation of the excitation forces and damping as assumed using ideal gas simplifications with compressibility factor corrections. In the current study, forced excitation due to diffuser vanes is considered for analysis.

Impeller Blade-Diffuser Vane Interaction

Giles [8] provides an extensive review of excitation mechanisms in bladed turbomachinery applications. See Figure which shows typical excitation mechanisms for turbomachinery blade rows. The interaction between centrifugal impeller blades and diffuser vanes can be characterized as a combination of potential and wake-rotor interaction. Wake interaction is due to wakes from upstream stator/rotor. Potential interaction is due to inviscid interaction between the stator vanes/rotor blades due to non-uniform pressure distributions on the vane/blade profiles. Potential interaction is typically seen in blade rows which have higher proximity such as impeller blade/diffuser vanes [9,10]. High Fidelity CFD analysis for determination of unsteady blade loading implicitly includes these interactions. The separation of wake/potential interaction is useful in determining stimulus variation as a function of vane/blade separation and can be an aid to developing correlations based on parametric studies using CFD or test campaigns. Aero-acoustic modes due to impeller diffuser interaction are also noted by Ramakrishnan et al. [11]. Evaluation of these modes and their influence is not within the scope of this paper.

.

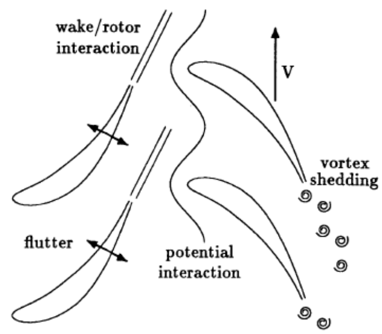

Figure 1: Source of unsteadiness in turbomachinery blade rows [Giles]

Unsteady blade loading on impeller blades can be detrimental when the frequency and phase of excitation pattern matches a corresponding structural mode of the impeller. This type of stator vane-rotor blade interaction is also termed as “Significant Minor Resonance” (see Kushner [12]) to distinguish from Major resonances (disk critical speed excitations) which can occur due to non axi-symmetric flow condition causing a standing wave excitation.

The excitability of a given mode to excitation depends on the mode shape and the phase of the excitation. For a certain combination of stator number of vanes (which dictate the phase of excitation) and rotor number of blades, specific mode shapes are excited and other types of mode shapes are not excited due to phase cancellation (even if there is a resonant condition i.e. frequency of excitation matches the natural frequency). This specific resonant condition is termed as “significant minor resonance” and the mode shapes which are excited belong to specific “nodal diameter” patterns depending on the stator/rotor vane counts. An algebraic representation for resonant condition is provided by Kushner [12] as follows:

$$
\begin{aligned}
|y \times S| \pm |z \times B| &= n \\
y \times S &= h \\
f_r &= y \times S \times w
\end{aligned}
\qquad (1)
$$

Here, B = number of rotating blades

S=number of stationary elements

f_r= natural frequency at speed, Hz

h = harmonic of speed

n = number of nodal diameter lines

y & z = integers>0

w = rotating speed, Hz

A similar criterion based on graphical representation is provided by Wildheim [13]. The graphical representation is termed as ZZENF (Zig Zag Excitation Natural Frequency) diagram and is also referred to as SAFE diagram (Singh et al. [14,15]) in literature. Graphical representation of Kushner's equation with Wildheim's interpretation is shown in Figure 2. The figure shows the case for a cyclically symmetric rotating structure with 11 blades. If this cyclically symmetric structure in analyzed using a sector model, a specific parameter called "harmonic index" can be generated which is an "integer that determines the variation in the value of a single degree of freedom at points spaced at a circumferential angle equal to the sector angle" [16]. This harmonic index correlates with "nodal diameter" patterns observed in the mode shapes of such structures. Note that harmonic index is typically a finite number which depends on the number of sectors considered for cyclic symmetry analysis (maximum harmonic index =int(number of sectors/2)) whereas nodal diameters can be infinite. (The relation between harmonic index and nodal diameters is provided in Equation (2) and taken from Ref [16]).

The relation between harmonic index and nodal diameter is given by:

$$d = m \cdot N \pm k \tag{2}$$

Here, d = nodal diameter,

N = number of sectors,

k = harmonic index,

$m = 0,1,2,3, \dots, \infty$

For the current example case with 11 blades (structure divided into 11 sectors), the maximum harmonic index of concern is 5. For a rotationally symmetric excitation from 16 stationary vanes, the harmonic index which will be excited is $|1 \times 16| - |11| = 5$ as per equation (1). This is also represented graphically using Wildheim's ZZENF (with a modification by expressing the y-axis as the number of stationary vanes instead of frequency) diagram as shown in Figure 2. For higher order excitations such as

2X of 16, harmonic index =1 is excited. Natural frequencies which intersect with excitation frequencies at these harmonic indices will be excited and any other interferences will be phase cancelled.

It is to be noted that interaction resonance indicated above specifically relates to perfect symmetric structures and symmetric excitation. In reality, deviations are expected in the geometry due to manufacturing tolerances. Material property variations may also break the symmetry. This may introduce “mistuning” in the system. See Pettinato et al. [17] for discussion on mistuning as related to centrifugal compressor impellers. In such cases, the actual response of the structure may include responses from harmonic indices which are phase cancelled in a symmetric structure. The excitation may also not be symmetric with varying interblade phase angle (example non-uniform stationary vane spacing or missing vanes). This “aerodynamic mistuning” may also excite modes within harmonic indices typically considered as phase cancelled. In this current study, the influence of mistuning –both geometry/material derived and aerodynamic is ignored and considered to be minimal.

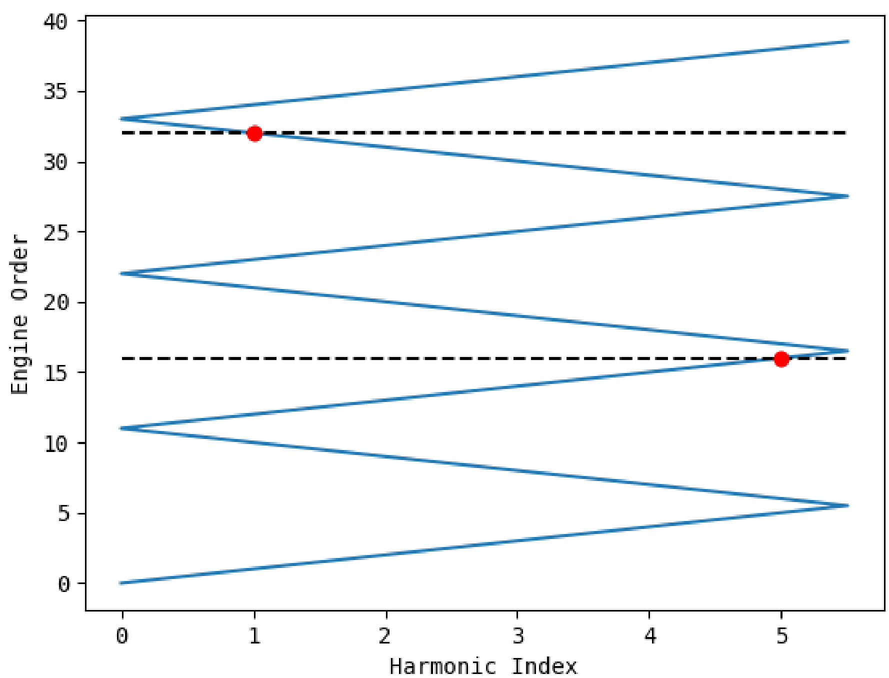

Figure 2: ZZENF diagram

References [18, 19, 20, 21] provide numerical computation using high fidelity CFD analysis of unsteady loading on impeller blades due to impeller-diffuser interaction. Estimation of unsteady loading on the impeller blades due to diffuser interaction using time-domain URANS CFD require a full wheel simulation or the use of transformation methods to adequately capture the flow across the rotor/stator domains with unequal pitch. ANSYS CFX [22] provides three methods for evaluation using transformation method, namely-profile transformation, time transformation and fourier transformation. Connell et al [23] provides a comparison of these methods with their application in analysis of a high pressure power turbine stage and a low pressure aircraft engine turbine stage. Alternately, frequency domain based method such as Non-Linear Harmonic Method (NLH) (See Vilmin et al [24] for details on the method) available through commercial software NUMECA FineTurbo25 provide a faster alternative for estimation of unsteady flow characteristics due to blade row interactions. This method transforms governing Navier-Stokes equations of fluid motion from time domain to frequency domain. The dominant frequencies of concern are the disturbance frequencies such as blade passing frequencies. The accuracy of the constructed solutions depends on the number of harmonics of the disturbance frequencies retained in the solution. Based on authors experience, the computational speed of analysis is much faster as compared to time domain methods. In the current analysis, NLH using NUMECA Fine™/ Turbo 18.2 is used to simulate the unsteady flow.

Centrifugal Compressor Stage Operating in sCO_2

To evaluate impeller-diffuser interaction in a sCO_2 application, an impeller from a last stage of a multi-stage inline compressor, Figure 3, designed for carbon capture and sequestration is considered. The overall process compresses the working fluid from 1 to 150 barA, with the inlet state to the last two stages being in the super-critical region. The compression process is configured to include five intercooling steps to maximize the iso-thermal efficiency and reduce the work of compression. This is accomplished using a three-body train to accommodate the substantial volume reduction.

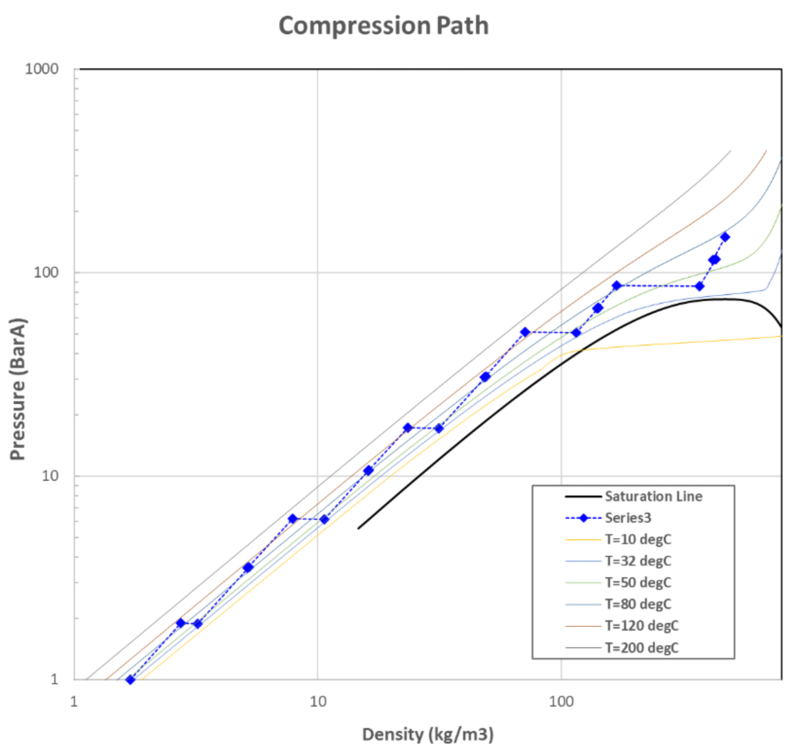

Figure 3: Overall Compression Path

The inlet conditions and non-dimensional aerodynamic parameters for the impeller are provided in Table 1. The impeller (see Figure 4) is a low flow coefficient impeller with design flow coefficient of 0.015. The number of impeller blades is 11 and the number of diffuser vanes is 16. The number of diffuser vanes of 14 was originally considered but it had insignificant separation margin from resonant excitation (significant minor resonance SMIR) for 3 nodal diameter mode. The flow coefficient of this stage is 0.013, which is not uncommon for supercritical stages in inline machines.

Table 1: Boundary conditions for the impeller

Flow Coefficient	0.013
Inlet Mach Number	0.56
Inlet Total Pressure	112.8 bar
Inlet Total Temperature	329.55 K
Mass Flow Rate	176.63 kg/s
Rotor Speed	6747 rpm

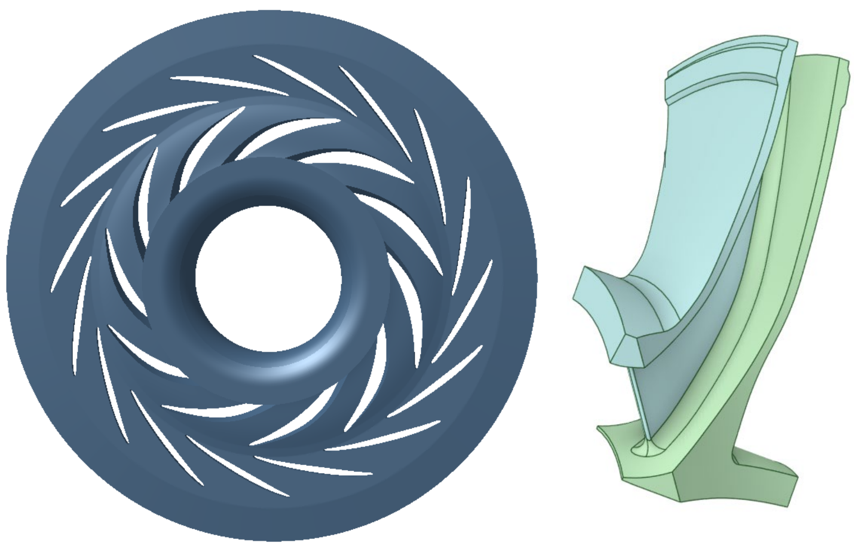

(a) (b)

Figure 4: (a) Impeller/Vaned Diffuser Sectional View (b) Impeller Sector Model

CFD Analysis Details

Unsteady loading on the blades is estimated using Non-Linear Harmonic (NLH) method [24] in Numeca Fine^{TM}/Turbo 18.2. The NLH method decomposes an unsteady fluid flow problem into key harmonics, such as blade passing frequencies, and solves those harmonics only to greatly reduce the computational time for an unsteady analysis. The impeller stage with the diffuser (one impeller blade passage and one diffuser vane passage) is modeled as shown in Figure 5. The CFD model has 1.096 x 10^6 nodes and 1.005 x 10^6 elements. Table based CO_2 gas properties are used in the CFD analysis to expedite the solver run time. Table properties were generated using TabGen software (part of Numeca/Cadence suite [25] of CFD software) which are based on NIST REFPROP [26] v10 database gas properties. Initially a steady state analysis is solved by imposing total pressure and temperature at the stage inlet and mass flow boundary condition at the outlet as per Table 1. Closure for the RANS model relied on the one equation Spalart-Allmaras turbulence model with wall functions.

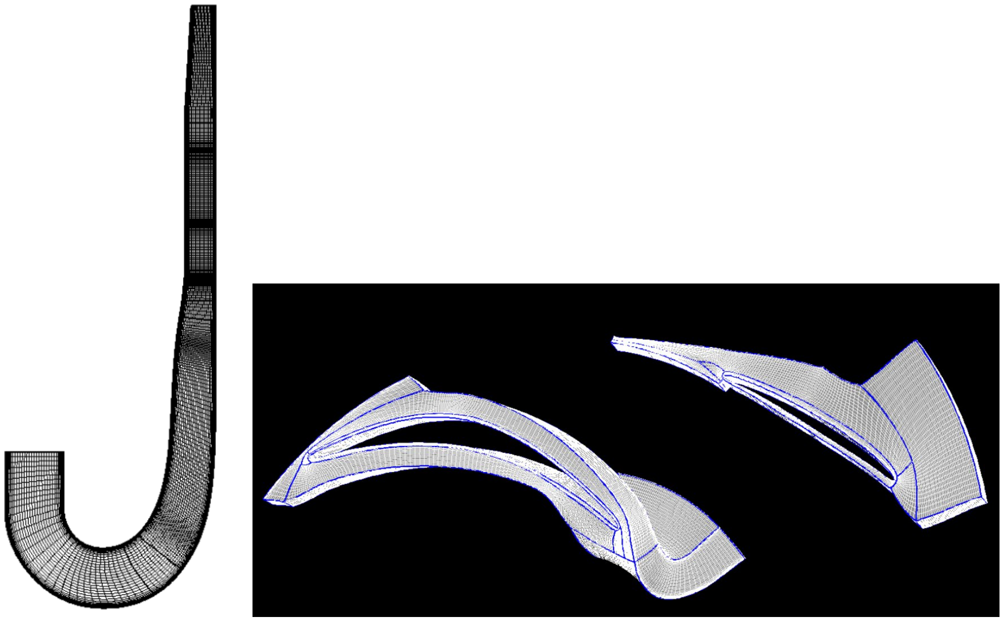

Figure 5: Fluid Mesh

NLH method is applied with the initial steady state solution. The model uses three harmonics and static pressure outlet boundary condition based on results from initial steady state solution. Figure 6 shows the harmonic pressure amplitudes in the blade passages at 50% span for 1st, 2nd and 3rd harmonics of vane passing frequencies. The maximum pressure amplitude for 1st harmonic is 5.16 bar, 2nd harmonic is 3.37 bar and 3rd harmonic is 1.83 bar. This shows that the higher harmonics are not negligible. However, Figure 6 also indicates that the higher harmonics are more localized and may not have much influence on the blade response as confirmed from the estimated structure response using Finite Element Analysis. The unsteady pressure loading on the blades is then transferred to the structural model of the impeller blades for harmonic response evaluation.

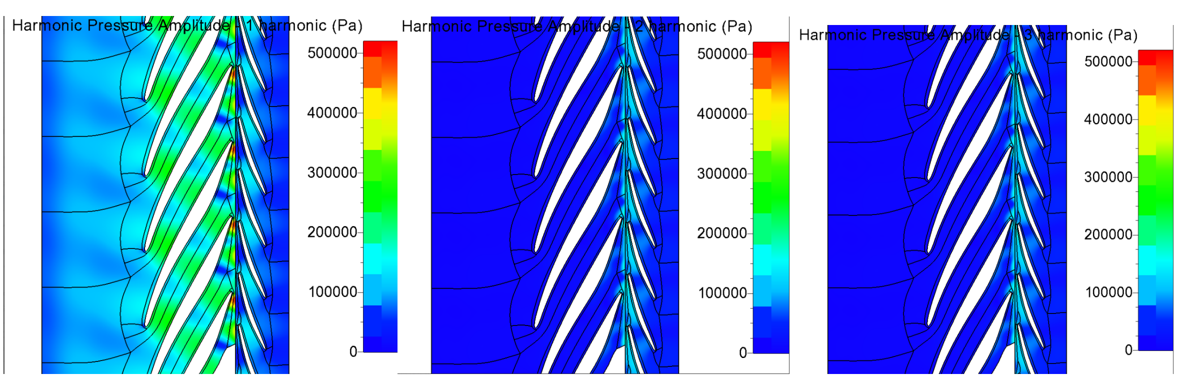

(a) (b) (c)

Figure 6: Harmonic Pressure Amplitude Blade-to-Blade view at 50% span (a) 1st Harmonic (b) 2nd Harmonic (c) 3rd Harmonic

Structural Analysis

Structural analysis is performed to estimate the natural frequencies of the impeller as well as to estimate the stresses due to steady and unsteadying loading. Analysis is performed using ANSYS Mechanical 2021. A sector model of the impeller blade passage is modeled as shown in Figure 7. Cyclic symmetry boundary conditions are used to solve for static, modal and harmonic analysis.

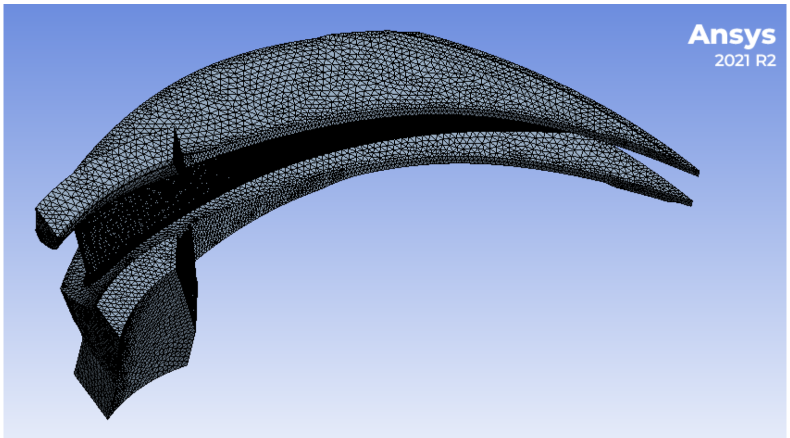

Figure 7: Sector model mesh

The closest natural frequency which can be excited due to 16EO is 5ND mode at 2589 Hz as shown in the ZZENF diagram in Figure 8. The separation margin is 44% from the 16X excitation due to diffuser vane interaction. As the separation margin is quite significant, the analysis speed for consideration in the current paper is increased to 9710 rpm to be in resonance with 5ND mode. This is done to demonstrate the stresses in the impeller in resonance. The steady and unsteady gas loading are based on aerodynamic analysis at 6746 rpm with the exception that the harmonic of consideration for unsteady loading is 16 times running speed of 9710 rpm.

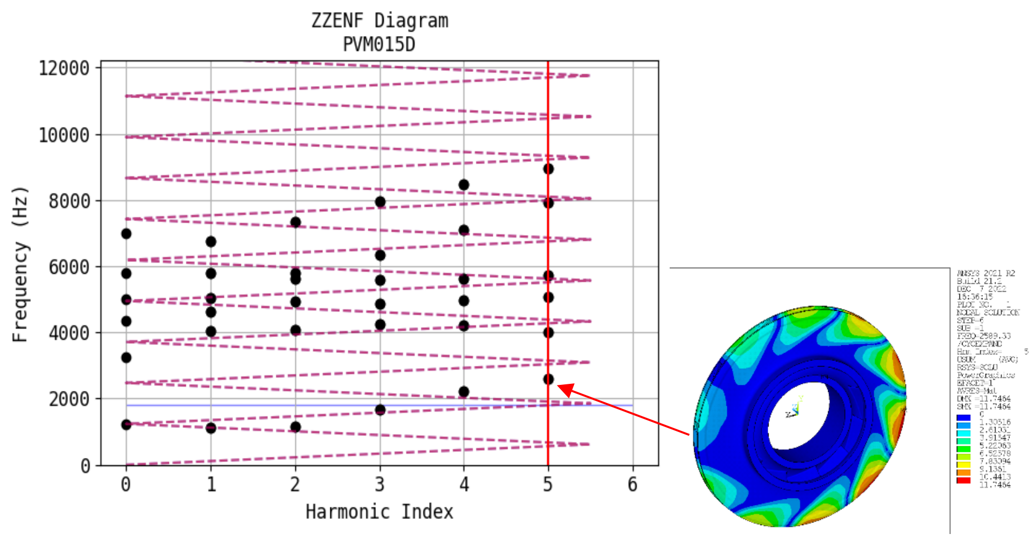

Figure 8: ZZENF diagram with mode shape for 5ND mode at 2589 Hz.

The steady state stresses on the impeller are dominated by the centrifugal stress. Figure 9 shows the equivalent Von-Mises stress distribution on the impeller due to centrifugal stress and gas bending model separately. The maximum stress using influence of gas loading only is about 22% as compared to maximum centrifugal stress. Note that gas loading stresses are, however, not additive to the centrifugal stress as seen in the estimated combined stresses (See Figure 10).

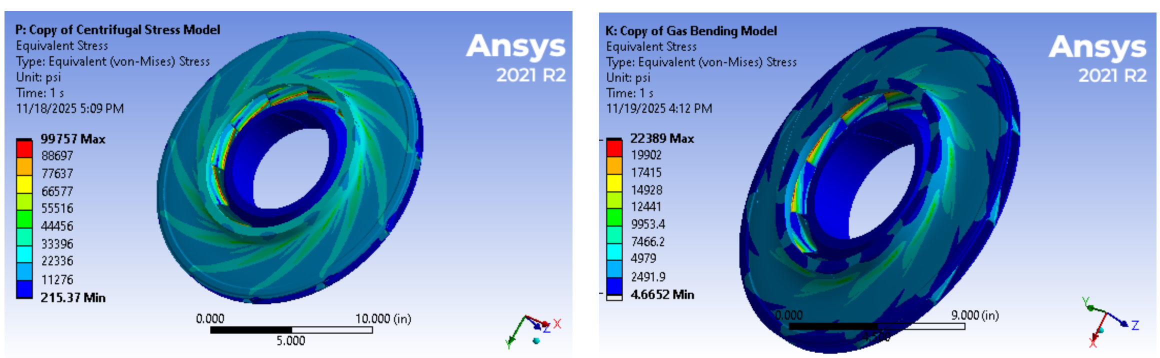

(a) (b)

Figure 9: (a) Centrifugal Stress (b) Steady Gas Loading

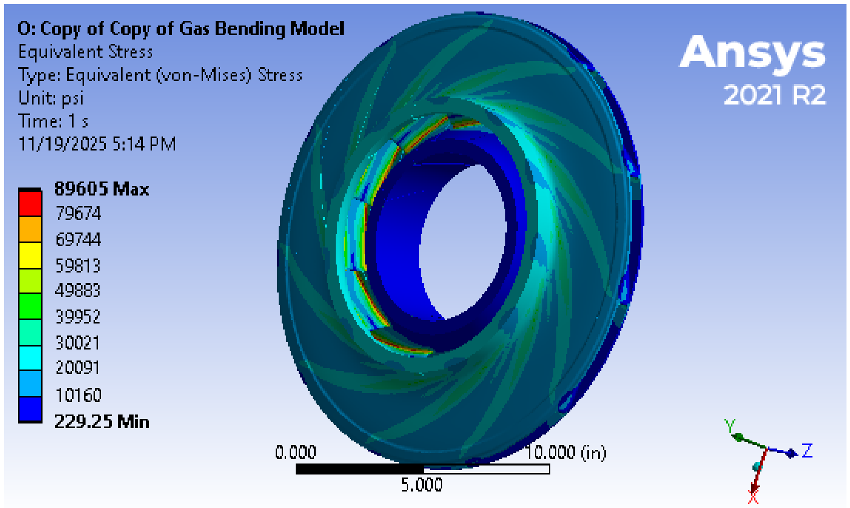

Figure 10: Combined Centrifugal + Steady Gas Loading

Unsteady loading obtained from the NLH CFD analysis is further transferred to the structural mesh in ANSYS for harmonic analysis (See Figure 11).

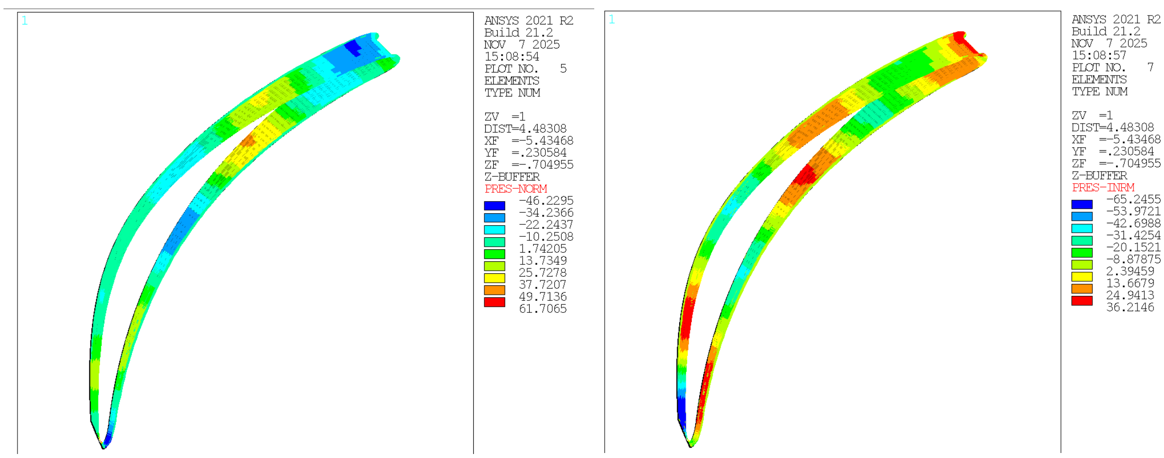

Figure 11: Harmonic pressure distribution (real and imaginary) on the blades

The structural response of the harmonic loading is limited by aerodynamic damping at resonance. Aerodynamic damping can be estimated by superimposing the structural motion at resonance in the CFD analysis and estimating the aerodynamic work. In the current study, aerodynamic damping of 0.3% is considered as a conservative estimate. This particular value is applicable to operation in air at atmospheric inlet conditions. Actual aerodynamic damping is expected to be proportional to gas density [27]. Figure 12 shows the harmonic response maximum equivalent stress distribution on the impeller during phase sweep i.e. during entire cycle of harmonic excitation.

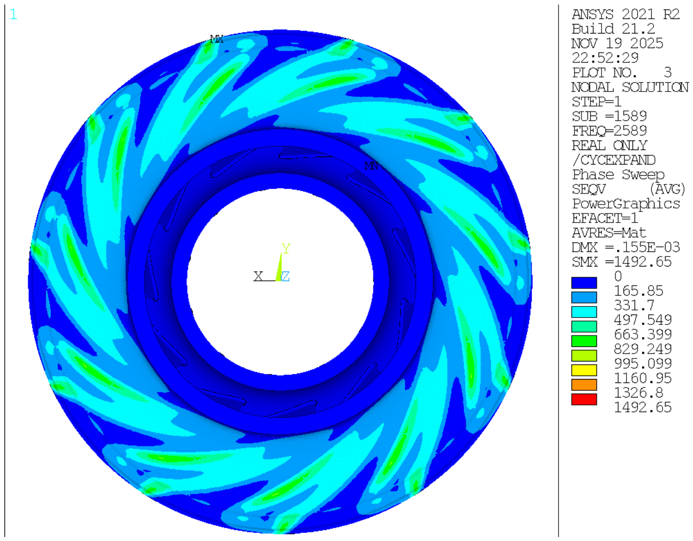

Figure 12: Maximum equivalent stress (phase sweep) using aerodynamic damping = 0.3% modal damping factor

High Cycle Fatigue Evaluation

The operation of impeller in resonance with diffuser interaction can lead to fatigue failure. The problem of fatigue in this situation is of the nature of high cycle fatigue as the number of stress cycles reach> 10^6 cycles within a few minutes of operation. Stress life method is considered for high cycle fatigue analysis with the results of alternating and mean stresses plotted on Goodman-Haigh diagram.

As the stresses on impeller are three dimensional, appropriate representation of mean and alternating stresses are required to correlate the stress data to fatigue test data (which is mostly uni-axial). For fatigue initiation, stresses on the free surface of the part are important as fatigue cracks usually start at the surface [28] . Stress condition is biaxial at the free surface. Alternating stress effects are considered using Von Mises equivalent stress representation as suggested by Sines [28]. The mean stress effect are considered using signed maximum principal stress. It is well known that fatigue strength reduction is not seen in compression. The results of alternating and mean stresses are plotted on a Goodman-Haigh diagram. Fatigue strength reduction due to tensile mean stress is considered. The method also places a limit based on yield strength (both tensile and compressive).

A high strength steel material with ultimate tensile strength of $\sigma_u = 135\ ksi$ and yield strength of $\sigma_y = 125\ ksi$ is considered for the impeller construction. The steady and alternating stresses for the current test case are plotted on Goodman-Haigh diagram as shown in Figure 13. The outer limits of the diagram are based on endurance limit with no fatigue strength modifiers and the inner limits are based on fatigue strength modifiers and safety factors. The stresses are shown to be acceptable for operation in resonance for this particular test case.

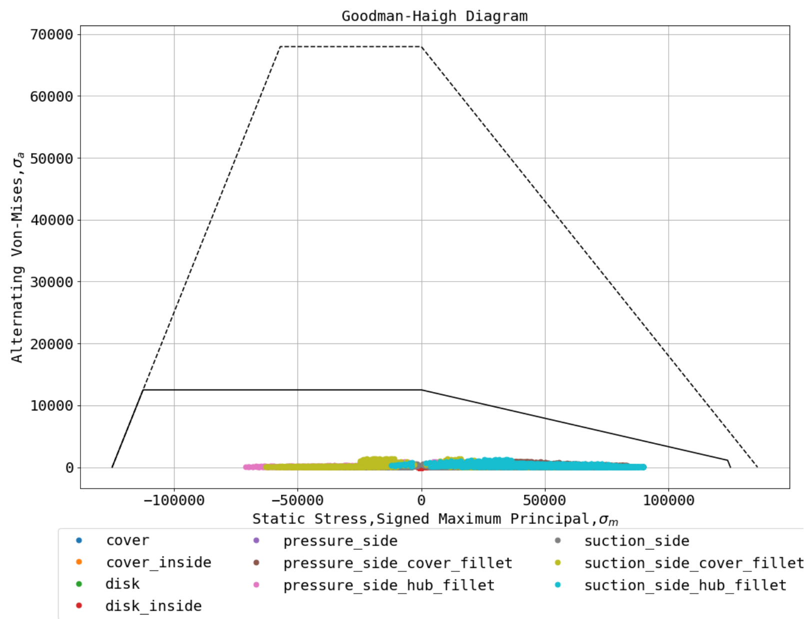

Figure 13: Goodman-Haigh Evaluation

Summary & Conclusions

A brief overview of aeromechanic failure modes in a centrifugal compressor impeller is provided. A major failure mode for typical application is due to interaction resonances with upstream and/or downstream stationary vanes. The likelihood of failure is due to the possibility of high stresses in the impeller at resonance and is of the nature of high cycle fatigue. The stresses can be managed by adequate separation margin from the resonant speeds or by evaluation of the stresses for high cycle fatigue and ensuring that they are within the limits of the selected material for impeller construction.

The paper presents a test case of impeller-diffuser interaction for a centrifugal compressor impeller operating in a sCO_2 application. For the design point of the application, the impeller is determined to be operating sufficiently away from the nearest excitation from vane passing frequency.

To review impeller stresses in resonance, the rotational speed of the impeller is increased to coincide with the resonant speed in the analysis. Unsteady loading (evaluated at design point) on the impeller blades are estimated using NLH CFD analysis and transferred to the structural model. The frequency of excitation is considered to be the resonant frequency (increased speed from design point) in the structural model. An assumed conservative value of aerodynamic damping is considered in the analysis. Maximum Von-Mises alternating stresses are determined from harmonic structural analysis.

Steady state stresses for the impeller are evaluated due to centrifugal effect from impeller rotation and gas loading due to operation at design point. The analysis indicates that centrifugal stresses and stresses due to steady gas loading require tensor addition (i.e. equivalent stresses are not additive).

High cycle fatigue evaluation of the impeller test case from these steady and alternating stresses indicates a safe operation even at resonance. This indicates that impeller blade construction and material selection for the impeller design is robust and less susceptible to failure from diffuser interaction for the selected test case. Although not within the scope of the current study, evaluation of aerodynamic damping and influence of cavity flows can provide further insight into resonant operation for this type of application.

REFERENCES

1. Haupt, U, Bammert, K, & Rautenberg, M., 1985, "Blade Vibration on Centrifugal Compressors: Blade Response to Different Excitation Conditions." Proceedings of the ASME 1985 International Gas Turbine Conference and Exhibit. Volume 4: Manufacturing Materials and Metallurgy; Ceramics; Structures and Dynamics; Controls, Diagnostics and Instrumentation; Education; Process Industries. Houston, Texas, USA. March 18–21, 1985. V004T13A007. ASME. https://doi.org/10.1115/85-GT-93
2. Haupt, U, Abdelhamid, AN, Kaemmer, N, & Rautenberg, M.,1986, "Excitation of Blade Vibration by Flow Instability in Centrifugal Compressors." Proceedings of the ASME 1986 International Gas Turbine Conference and Exhibit. Volume 1: Turbomachinery. Dusseldorf, West Germany. June 8–12, 1986. V001T01A115. ASME. https://doi.org/10.1115/86-GT-283
3. Abraham Engeda, 2012, "Rotating stall in centrifugal compressor and its effect on inducing vibration," AIAA 1994-2973. *30th Joint Propulsion Conference and Exhibit*. June 1994. https://doi.org/10.2514/6.1994-2973
4. Curtin, A, Berdanier, RA, Kunz, RF, & Jonson, ML. 2019, "Evaluating Splitter Blade Designs to Avoid Impeller Failure in a High-Speed Unshrouded Centrifugal Compressor." Proceedings of the ASME Turbo Expo 2019: Turbomachinery Technical Conference and Exposition. Volume 7A: Structures and Dynamics. Phoenix, Arizona, USA. June 17–21, 2019. V07AT36A015. ASME. https://doi.org/10.1115/GT2019-91359
5. Konig, S., Petry, N. and Wagner, N., 2009, “Aeroacoustic Phenomena In High Pressure Centrifugal Compressors-A Possible Root Cause For Impeller Failures,” Turbomachinery Symposium, Texas A&M University, https://hdl.handle.net/1969.1/163083
6. Petry, N, Benra, FK, & Koenig, S. "Experimental Study of Acoustic Resonances in the Side Cavities of a High-Pressure Centrifugal Compressor Excited by Rotor/Stator Interaction." Proceedings of the ASME Turbo Expo 2010: Power for Land, Sea, and Air. Volume 7: Turbomachinery, Parts A, B, and C. Glasgow, UK. June 14–18, 2010. pp. 2339-2351. ASME. https://doi.org/10.1115/GT2010-22054
7. Kushner, F., Pettinato, B., Pechulis, M., Thorat, M., 2024, “Modal Analysis and Resonance Avoidance of Bladed Disks,” Proceedings of Turbomachinery Symposium, Texas A&M University, https://hdl.handle.net/1969.1/1582470

8. Giles, M., 1991, “UNSFLO: A Numerical Method for the Calculation of Unsteady Flow in Turbomachinery,” GTL Report 205, Cambridge, Mass. : Gas Turbine Laboratory, Massachusetts Institute of Technology http://hdl.handle.net/1721.1/104744

9. Sanders, A.J., and Fleeter, S., 1998, “Potential Field Interactions in a Low-Speed Centrifugal Compressor”, AIAA Journal of Propulsion and Power, Vol. 14, No. 6, pp. 925-933.

10. Sanders, A.J., Carnell, W. F., Jr., Oakes, W., Lawless, P. B., and Fleeter, S., 2001, “Characteristics of Potential Forcing Functions in High Speed Centrifugal Compressors”, AIAA Paper 2001-3620.

11. Ramakrishnan, K, Richards, SK, Moyroud, F, & Michelassi, V. "Multi-Blade Row Interactions in a Low Pressure Ratio Centrifugal Compressor Stage With a Vaned Diffuser." Proceedings of the ASME 2011 Turbo Expo: Turbine Technical Conference and Exposition. Volume 6: Structures and Dynamics, Parts A and B. Vancouver, British Columbia, Canada. June 6–10, 2011. pp. 1321-1329. ASME. https://doi.org/10.1115/GT2011-45932

12. Kushner, F., 1979, “Disc Vibration - Rotating Blade and Stationary Vane Interaction,” ASME Paper No. 79-Det-83.

13. Wildheim, S. J. (December 1, 1979). "Excitation of Rotationally Periodic Structures." ASME. J. Appl. Mech. December 1979; 46(4): 878–882. https://doi.org/10.1115/1.3424671

14. Singh, Murari P.; Vargo, John J.; Schiffer, Donald M.; Dello, James D. (1988). Safe Diagram - A Design And Reliability Tool For Turbine Blading.. Texas A&M University. Turbomachinery Laboratories. Available electronically from https : / /hdl .handle .net /1969 .1 /163593.

15. Singh, M. P., Thakur, B. K., Sullivan, W. E., Donald, G., 2003, “Resonance Identification for Impellers”, Proceedings of the 32nd Turbomachinery Symposium, Turbomachinery Laboratory, Texas A&M University, College Station, Texas. https://doi.org/10.21423/R1XM17

16. ANSYS® Mechanical APDL, Release 2024 R1, Help System, Cyclic Symmetry Analysis Guide, Ansys, Inc.

17. Pettinato, Brian; Wang, Yongxin; Griffin, Jerry; Feiner, Drew; Echols, Brian; Cushman, Michael (2013). Experimentally Based Statistical Forced Response Analysis for Purpose of Impeller Mistuning Identification. Turbomachinery Laboratory, Texas A&M Engineering Experiment Station. Available electronically from https://hdl.handle.net/1969.1/172623

18. Gould, KA, Tan, CS, & Macrorie, M. "Characterization of Unsteady Impeller-Blade Loading in a Centrifugal Compressor With a Discrete-Passage Diffuser." *Proceedings of the ASME Turbo Expo 2007: Power for Land, Sea, and Air*. *Volume 6: Turbo Expo 2007, Parts A and B*. Montreal, Canada. May 14–17, 2007. pp. 1781-1790. ASME. https://doi.org/10.1115/GT2007-28002

19. Lusardi, C., 2012, “Characterization of Unsteady Loading Due to Impeller Diffuser Interaction in Centrifugal Compressors,” M.S. thesis, Massachusetts Institute of Technology, Cambridge, MA.

20. Toni, L., Moyroud, F., Ramakrishnan, K., Michelassi, V. and Schurr, E., 2017. Prediction and validation of high-performance centrifugal compressor impeller forced response. In *12 th European Conference on Turbomachinery Fluid dynamics & Thermodynamics*. European Turbomachinery Society.

21. Walton, E. J., and Tan, C. S. (April 5, 2016). "Forced Response of a Centrifugal Compressor Stage Due to the Impeller–Diffuser Interaction." ASME. J. Turbomach. September 2016; 138(9): 091004. https://doi.org/10.1115/1.4032838

22. ANSYS® CFX, Release 2024 R1, Help System, Transient Blade Row Modeling Theory , Ansys, Inc.

23. Connell, S, Braaten, M, Zori, L, Steed, R, Hutchinson, B, & Cox, G. "A Comparison of Advanced Numerical Techniques to Model Transient Flow in Turbomachinery Blade Rows." Proceedings of the

ASME 2011 Turbo Expo: Turbine Technical Conference and Exposition. Volume 7: Turbomachinery, Parts A, B, and C. Vancouver, British Columbia, Canada. June 6–10, 2011. pp. 1241-1250. ASME. https://doi.org/10.1115/GT2011-45820

24. Vilmin, S, Lorrain, E, Hirsch, C, & Swoboda, M. "Unsteady Flow Modeling Across the Rotor/Stator Interface Using the Nonlinear Harmonic Method." Proceedings of the ASME Turbo Expo 2006: Power for Land, Sea, and Air. Volume 6: Turbomachinery, Parts A and B. Barcelona, Spain. May 8–11, 2006. pp. 1227-1237. ASME. https://doi.org/10.1115/GT2006-90210
25. Numeca Fine™/Turbo, User Manual Fine/Turbo v. 17a. NUMECA International, Brussels Belgium.
26. Lemmon, E.W., Bell, I.H., Huber, M.L., McLinden, M.O. NIST Standard Reference Database 23: Reference Fluid Thermodynamic and Transport Properties-REFPROP, Version 10.0, National Institute of Standards and Technology, Standard Reference Data Program, Gaithersburg, 2018. doi: https://doi.org/10.18434/T4/1502528
27. Toni, L., Gatta, G., Moyroud, F., Guglielmo, A., Rubino, D.T. and Ramakrishnan, K., 2016," Aero-damping measurements and computation in a full-scale multistage centrifugal compressor", Proceedings of Turbomachinery Symposium, Texas A&M University, https://hdl.handle.net/1969.1/159794
28. Sines, G., and Ohgi, G. (April 1, 1981). "Fatigue Criteria Under Combined Stresses or Strains." ASME. J. Eng. Mater. Technol. April 1981; 103(2): 82–90. https://doi.org/10.1115/1.3224995